PROCEEDINGS OF SCIENCE

Time-Resolved Fast-Neutron Imaging with a Pulse-Counting Image Intensifier

Volker Dangendorf[*], Ronald Lauck, Frank Kaufmann

Physikalisch-Technische Bundesanstalt
Braunschweig, Germany
E-mail: `volker.dangendorf@ptb.de` and `frank.kaufmann@ptb.de`

Juergen Barnstedt

Institut fuer Astronomie und Astrophysik, Univ. Tuebingen
Tuebingen,, Germany
E-mail: `barnstedt@astro.uni-tuebingen.de`

Amos Breskin

Weizmann Institute of Science
Rehovot, Israel
E-mail: `amos.breskin@weizmann.ac.il`

Ottmar Jagutzki

Institut fuer Kernphysik, Univ. Frankfurt
Frankfurt/M, Germany
E-mail: `jagutzki@atom.uni-frankfurt.de`

Michael Kraemer

Gesellschaft für Schwerionen (GSI)
Darmstadt, Germany
E-mail:m..kraemer@gsi.de

David Vartsky

NRC Soreq
Yavne, Israel
E-mail: `david@soreq.gov.il`

[*] Speaker

A new imaging method that combines high-efficiency fast-neutron detection with sub-ns time resolution is presented. This is achieved by exploiting the high neutron detection efficiency of a thick scintillator and the fast timing capability and flexibility of light-pulse detection with a dedicated image intensifier. The neutron converter is a plastic scintillator slab or, alternatively, a scintillating fibre screen. The scintillator is optically coupled to a pulse counting image intensifier which measures the 2-dimensional position coordinates and the Time-Of-Flight (TOF) of each detected neutron with an intrinsic time resolution of less than 1 ns. Large-area imaging devices with high count rate capability can be obtained by lateral segmentation of the optical readout channels.

1. Introduction

Energy-resolved fast-neutron radiography is a promising method for element sensitive imaging of low-Z materials which cannot be resolved by standard X-ray or thermal neutron techniques. Fast-neutrons have a high penetration power and, due to the specific structures (resonances) in the neutron cross sections of elements like C, N or O in the MeV range, the spatial distribution of those elements e.g. in air cargo containers or luggage may be resolved by this method. A prerequisite for the application of the method is the possibility to obtain two-dimensional neutron transmission images in selected narrow energy ranges – either in a sequence of several images with selected quasi-monoenergetic neutron beams [1] or, alternatively, with a pulsed, broad energy neutron beam and the application of Time-Of-Flight (TOF) methods for energy selection [2, 3].

In recent years we have investigated various imaging techniques based on position sensitive gaseous detectors with pulse-counting electronic readout [4] and, alternatively, on scintillators with image-integrating optical read out [3, 5, 6]. The gas detectors have good time resolution but suffer from low neutron detection efficiency, while the scintillator systems exhibit high detection efficiencies and high rate capability but suffer from relatively poor time resolution. In this work we present a method which combines the high efficiency of a thick scintillator with the intrinsically good time resolution of the pulse counting method.

2. The Fast-Neutron Camera

Previously, we described a method for time-resolved fast-neutron imaging using a scintillator screen (or a scintillating fibre screen) whose light is read out via several time-gated imaged intensifiers and CCD cameras [3, 5, 6]. The advantage of this method is, that due to the integrative readout with CCDs there is no limitation on the neutron count rate. However, the drawback is the rather limited time resolution (of the order of 8 to 15 ns) which implies large source-detector distances to obtain the required energy resolution. Furthermore, depending on the number of different energy bins required to measure the distribution of e.g. three different elements, six gated intensified CCD cameras are required, each adjusted to a selected TOF window and viewing the same part of the scintillator screen. In this contribution we propose to

replace the gated intensifier by a pulse-counting intensifier. This enables individual neutron counting by detecting the scintillation light of each neutron which is converted in the screen, thereby permitting the determination of its position and TOF.

2.1. Pulse Counting Image Intensifier (PCII)

Well known examples of pulse counting position-sensitive optical detectors are the cross wire PMTs [7] or pixel-anode PMTs [8]. Fast-neutron imaging with fast plastic or liquid scintillators suffers from the low light yield per detected neutron and the small solid angle for light detection, caused by the necessity of using a demagnifying lens coupling between the scintillator and the optical detection system. Therefore, on average, only a small number of photons per converted neutron reach the photocathode and the signals of the light detector are caused mainly by single or few photoelectrons. Therefore we have applied here a technique developed in 1994 using a standard proximity-focussed cascaded multi-channel-plate (MCP) image intensifier with a special anode [9,10]. This anode, made of highly resistive material instead of the standard phosphor for optical readout, allows to determine the position of the travelling electron cloud, emerging from the last MCP, by a suitable read-out electrode placed outside the vacuum tube (Fig. 1). The fast timing signal is derived from the anode of the last MCP. To achieve good position and time resolution, even with single photo electrons, saturated pulses are obtained by using a z-stack of three MCP's for electron multiplication. The diameter of the PCII used in our experiment is 25 mm. The readout electrode is a double-sided, pad-structured PC-board using a delay line for position coding. The readout method is described in greater detail in [4].

With this readout scheme position resolutions of 87 μm and 123 μm (fwhm) were recorded with single photoelectrons for X and Y coordinates, respectively; X and Y are the respective front- and rear-side of the readout board.
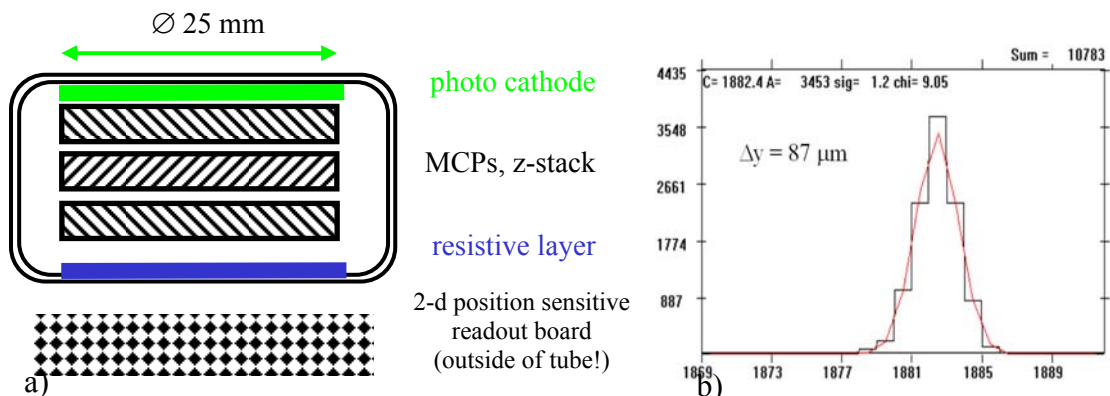

Fig.1: a) Schematics of the PCII, a 25 mm diameter Proxitronic Proxifier [11] with an inner resistive anode which replaces the phosphor of the standard intensifier and a 2-D readout board placed outside the vacuum vessel.
b) With a delay line readout a resolution of 87 μm (fwhm) was obtained for single photoelectrons.

2.2. Modular Neutron Detector with Multiple PCII

Due to the low light yield of neutrons in fast plastic or liquid scintillators and the small solid angle of the optical detection system the maximum size of the scintillator screen viewed by a 25 mm image intensifier should not be larger than about 100 cm^2. The solid angle for light detection (g) is obtained by:

$$g = \frac{\Delta\Omega}{4\pi} \cong \frac{1}{16n^2} \frac{m^2}{F\#^2 (1+m)^2}$$

The size of the largest square inside a 25 mm diameter tube is about 17 mm, which sees a square piece of the scintillator of 100 mm edge length. This results in a demagnification of $m =$ 0,17 With a fast lens ($F\# \sim 1.0$) and a refractive index of the scintillator of $n = 1.55$ we obtain from this equation a solid angle of $g \sim 5.4*10^{-4}$. For an 8 MeV neutron the average knock-on proton energy is about 4 MeV. A plastic scintillator will emit 4300 photons/MeV for these protons, or $N = 17500$ photons/neutron. With a photocathode quantum efficiency $QE = 20$ % we obtain the number of photoelectrons/neutron as : $N_e = N * g * QE$. In this example we obtain on the average 1.9 photoelectrons   per converted neutron !

A practical detector would naturally require a much larger area: typically one would need a 50 x 50 cm detector or a rectangular detector of 20 cm x 1 m. Such a detector must be assembled from a number of smaller units, e.g. as indicated in fig. 2.
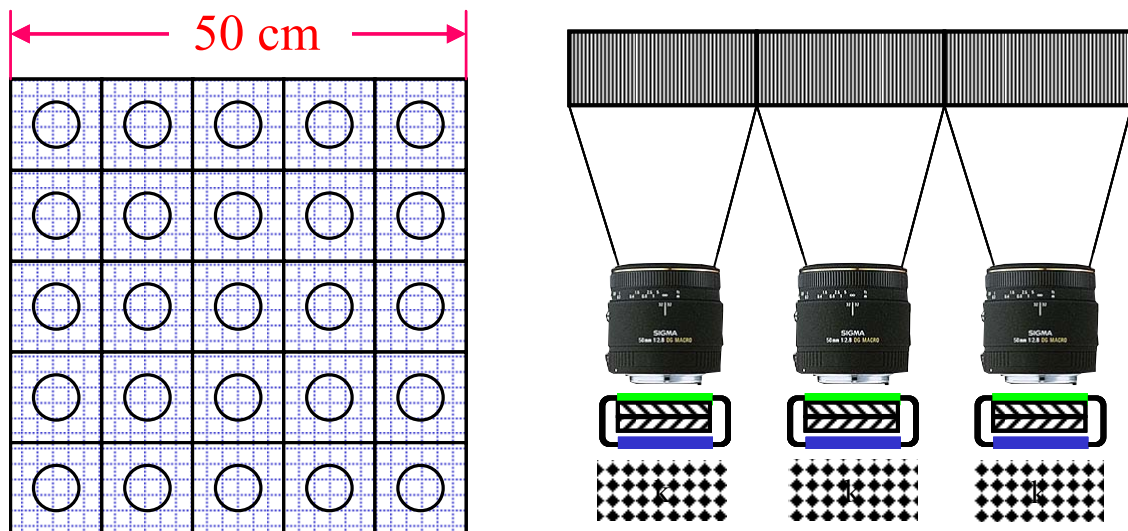

Fig.2: Example of an 50 x 50 cm^2 large scintillating fibre screen, read out by an array of 25 smaller PCII's, each covering an area of 100 cm^2.

2.3. Set up for the Test Experiment

For testing the principle we have assembled a detector consisting of a 10 mm thick BC400 scintillator slab. The optical read out consisted of a large aperture lens (focal length f = 120 mm, $F\#$ = 0.95) and a PCII with a photocathode diameter of 25 mm. Fig. 3 shows a schematic view of the detector. The electronic readout was similar to the one described in [4], using the ACAM-TDC and a data acquisition system based on "Satan" [12].

With this detector we have performed measurements at the neutron beam facility of PTB, similar to the ones described in [3, 4]. The neutron beam was produced by a pulsed 12 MeV deuterium beam that strikes a 3 mm thick Be target. The distance between neutron source (Be target) and detector was 6 m and the sample was placed directly on the input window in front of the scintillator.
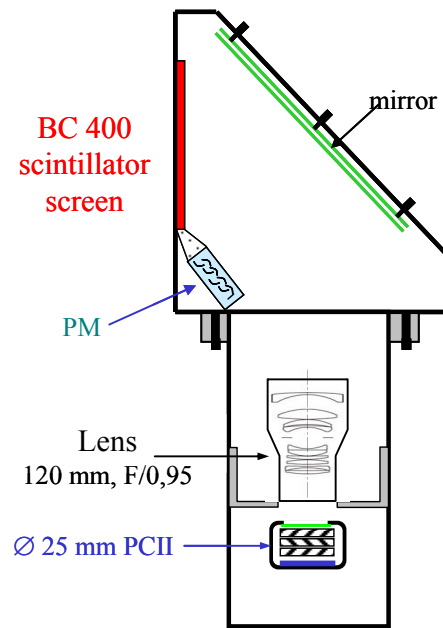
Fig.3: Schematic view of the neutron imaging system used to test the method of an optical readout with a pulse-counting image intensifier.

3. Results and Discussion of the Fast-Neutron Camera

3.1. Imaging without TOF

Fig. 4 shows the neutron image of a sample consisting of carbon rods of various diameters and lengths, as well as a steel wrench. For this image neutrons in the whole available energy range (1 – 10 MeV) were utilized. The acquisition time per image was ~8 h at an average rate of ~100 kHz.

The visible part of the screen has a diameter of ~10 cm. Close to the edge we see distortions which are due to the insufficient size of the resistive anode inside the intensifier and the influence of a metal ring close to this layer.

The small figures to the right show:

top: flat image, obtained without a sample in the beam, center: uncorrected image of the object and bottom and large image in the center-left: flat-field corrected image of the sample. The horizontal and vertical streaks in the flat field and the uncorrected image are due to nonlinearities of the readout circuit and to cross-talk in the readout electronics. These structures disappear completely in the corrected image.
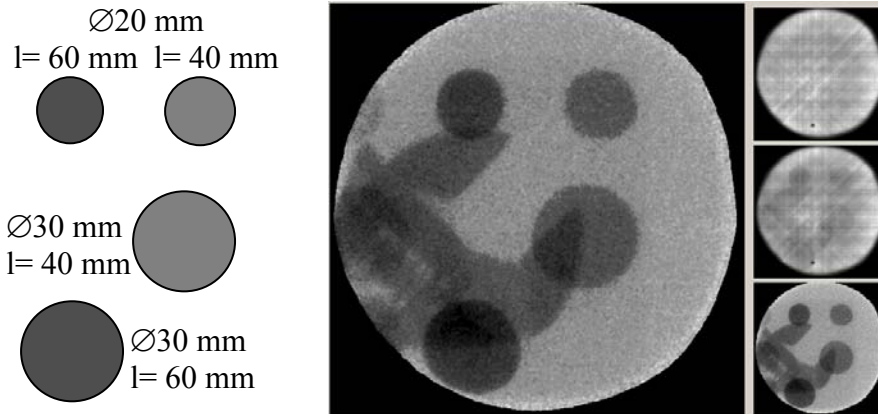
Fig.4: Neutron image of various carbon rods and a steel wrench, obtained in a broad energy neutron beam (1 – 10 MeV) . The C-rods have diameters of 30 mm and 20 mm and a length of 60 mm and 40 mm.

3.2. Time resolution and TOF Spectra

Fig. 5 shows the Time-Of-Flight (TOF) spectra measured with the neutron camera at 6 m distance from the Be target. The black curve in fig. 5a shows the TOF Spectrum without sample object while the red curve is obtained behind a 40 mm long C-rod. The graph in fig. 5 b shows the details of the peak induced by the gamma rays (γ-peak). Neglecting the intrinsic time resolution of the PCII the width and form of the γ-peak are determined by a superposition of the width of the ion pulse (ca 2 ns), the energy-dependent flight-time through the scintillator (<1 ns above 2 MeV) and the temporal probability distribution to detect the first photon produced by a converted neutron in the PCII. As mentioned above, the majority of the detected neutrons generate only a small number (1-2) of photoelectrons. In this case the mentioned probability distribution follows closely the light decay curve of the scintillator which is clearly visible in
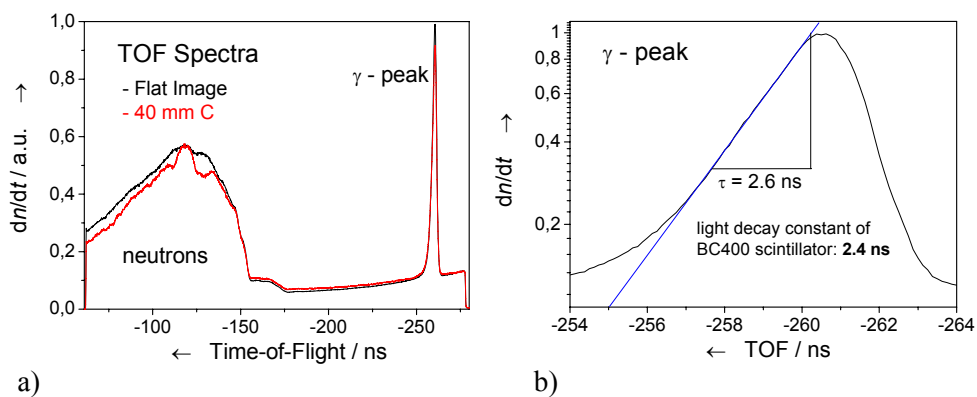

Fig.5: a) Neutron TOF spectra with (red curve) and without (black curve) carbon sample. b) shows details of the γ-peak. The form of the γ-peak is predominantly determined by the time structure of the deuterium beam and the light decay time of the scintillator

fig. 5b as an exponential tail with a decay constant of 2.6 ns towards longer TOF values. Clearly, with a better light collection efficiency, e.g. with a conical fibre-optical taper coupling (instead of an optical lens), the influence of the scintillator light decay will be much smaller.

3.3. Spectroscopic Imaging

Resonance imaging requires the comparison of neutron images obtained at different energies. The measurement of the spatial distribution of a single element in a complex sample requires two radiographs at selected energies. Here we test the method with carbon, exploiting the resonances in the 6.5 – 8.2 MeV region (for more details see [3, 4]). The red curve in fig. 6 shows the published ENDF-B6 total neutron cross section of carbon as function of neutron TOF under the described experimental conditions. The experimental structure of the cross section was determined from the ratio of the black curve (without sample) and red curve (with carbon sample) of fig. 5a. This ratio is plotted in fig. 6a as black curve. Two images are derived from the list-mode data with specific window conditions on the neutron TOF, analogous to "ON" and "OFF" resonance measurements (see red and blue bar in fig. 6a). The images, after being "flat-field" corrected, are displayed in fig. 6b. Of course, all the radiographed objects (carbon and steel) are visible in these images. In the next step, these images are smoothed to reduce the statistical "pixel" noise and the ratio of the two images is calculated, pixel by pixel. Fig. 7 shows the resulting image. Only the carbon remains visible while the steel, whose neutron cross section is rather flat in this energy region, disappears. Also two carbon rods with a length of 20 mm, which are barely distinguishable in the previous images, now appear clearly on the left side of the sample.
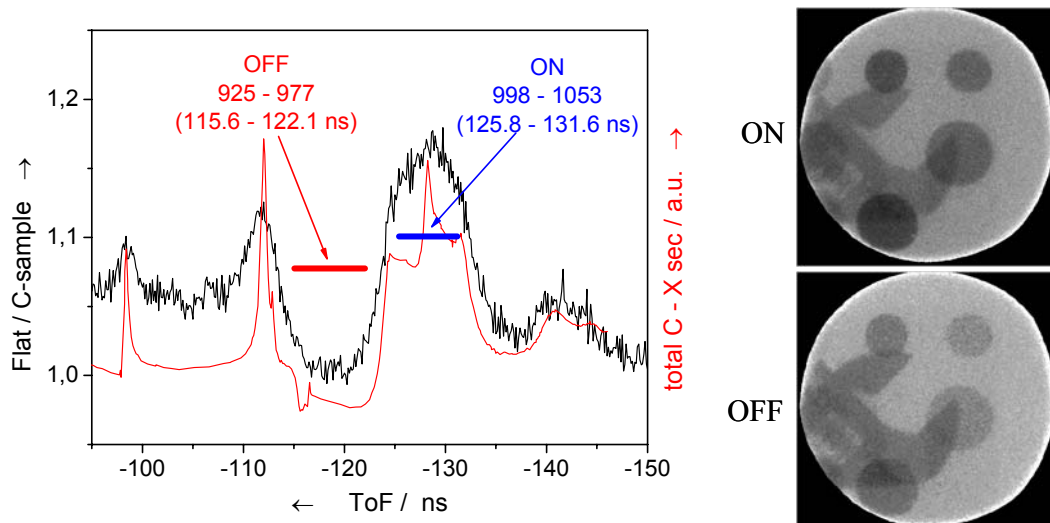

Fig.6: a) Ratio of the neutron TOF data of fig.5 a, "without" / "with" carbon sample. The red curve in fig.6 a. shows the total cross section of carbon. The red and blue bar indicate the TOF windows used for ON and OFF resonance images. b) shows the images collected from the list-mode file with appropriate TOF conditions.
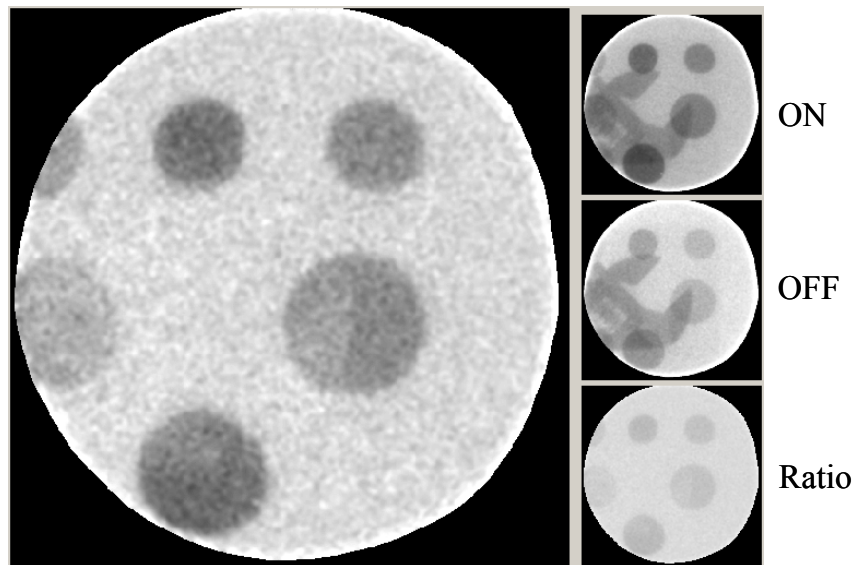
Fig.7: Carbon distribution in the sample, utilising neutron resonance imaging. At the right side the radiographs at energies "On" and "Off" the resonance are shown (top and center). The images at bottom right and the enlarged one on the left show the pixel-by-pixel ratio of the two images just mentioned, which represents the carbon distribution in the sample.

4. Conclusion

We presented a new method for time-resolved fast neutron imaging with a pulse-counting image-intensifier. While the time resolution is superior to previously presented methods [4, 6] the position resolution is comparable to the other methods. However, the intrinsic weakness of the counting method is the rate capability. Following the hypothetical estimates of Vartsky [6], the neutron flux incident on a detector which is required for a reliable detection of threat quantities of explosives is about 1×10^4 n/s/cm^2 in each energy bin. If we assume six energy bins, which account for about 50 % of the total neutron flux and a detection efficiency of 15 %, the overall rate per detector cell (100 cm^2 area) is about 1.8 MHz. This rate is quite feasible in such a detector element not only by the intensifier itself but also by a dedicated data acquisition system. In contrast to our laboratory device where list-mode storage is employed one would of course reduce the data stream already during run time via front-end online analysis to the required number of radiographic images in selected energy ranges.

Acknowledgment

References

[1] G. Chen , R. C. Lanza, *Fast Neutron Resonance Radiography for Elemental Imaging: Theory and Applications*, IEEE-NS 49, (2002), p.1919 - 1924
see also: R. C. Lanza, *Fast Neutron Resonance Radiography for Threat Interdiction:Technical Challenges and Preliminary Results*, these proceedings

[2] J.C. Overley, *Explosives detection through Fast-Neutron Time-of-Flight Attenuation Measurements, Nucl. Instr. and Meth*. B 99 (1995) 728, see further references in [6]

[3] V. Dangendorf, G. Laczko, C. Kersten, O. Jagutzki, U. Spillman, *Fast Neutron Resonance Radiography in a Pulsed Neutron Beam*, in: Neutron Radiography**,** Proceedings of the Seventh World Conference, Rome, Italy, September 15-21, 2002, Vol. 7, P. Chirco, R. Rosa (Eds.) ENEA, Public Relations Department-Communication Unit, Rome, 2005, pp. 383 – 398, see also: http://www.arxiv.org/abs/nucl-ex/0301001

[4] V. Dangendorf, G. Laczko , M. Reginatto, D. Vartsky, M. Goldberg, I. Mor, A. Breskin, R. Chechik, *Detectors for Time-of-Flight Fast Neutron Radiography: 1. Neutron Counting Gas Detector,* Nucl. Instrum. Meth. A 542 (2005) 197-205, see also: http://www.arxiv.org/abs/physics/0408074

[5] Ilan Mor, MSc - Thesis, Soreq 2006, extracts to be published

[6] D. Vartsky, *Prospects of Fast-Neutron Resonance Radiography and its Requirements for Instrumentations*, these proceedings

[7] Position-Sensitive PMT with Crossed Wire Anodes, http://sales.hamamatsu.com/

[8] Photonis Multi-Channel PMTs, http://www.photonis.com/Photomultiplier/ multichannel_pmt.htm

[9] O.Jagutzki, J. U. Spillmann, L. Spielberger, V. Mergel, K. Ullmann-Pfleger, M. Grewing, H. Schmidt-Boecking, *Fast-position and time-sensitive readout of image intensifiers for single-photon detectio*n, in: Ultraviolet and X-Ray Detection, Spectroscopy and Polarimetry III, S. Fineschi, B. E. Woodgate, R. A. Kimble, Eds. Proc. SPIE Vol. 3764, (1999), p. 61-69

[10] J. Barnstedt, M. Grewing, *Development and characterisation of a visible light photon counting imaging detector system*, Nucl. Instrum. and Meth. A 477 (2002) 268 – 272

[11] Proxitronic, Robert-Bosch-Str. 34, D-64625 Bensheim, web: www.proxitronic.de

[12] M. Kraemer, Listmode data evaluation with SATAN, http://www-aix.gsi.de/~bio/docs/satan/ pro/docs/satan.html